REPORT DOCUMENTATION PAGE

Form Approved
OMB No. 0704-0188

1. AGENCY USE ONLY (Leave blank)	2. REPORT DATE	3. REPORT TYPE AND DATES COVERED
	11 Feb 94	FINAL REPORT 90DEC15 - 93DEC15

4. TITLE AND SUBTITLE
Controlling Combustion and Maximizing Heat Release in a Reacting Compressible Free Shear Layer

5. FUNDING NUMBERS
PE - 61102F
PR - 2308
SA - BS
C - F49620-91-C-0020

6. AUTHOR(S)
Dr. David Nixon, Dr. Laurence R. Keefe

7. PERFORMING ORGANIZATION NAME(S) AND ADDRESS(ES)
Nielsen Engineering & Research, Inc.
526 Clyde Avenue
Mountain View, CA 94043-2212

8. PERFORMING ORGANIZATION REPORT NUMBER
TR-476
AFOSR-TR- 94 0167

9. SPONSORING/MONITORING AGENCY NAME(S) AND ADDRESS(ES)
AFOSR/NA
110 Duncan Avenue, Suite B115
Bolling AFB DC 20332-0001

10. SPONSORING/MONITORING AGENCY REPORT NUMBER
Contract No.
F49620-91-C-0020

11. SUPPLEMENTARY NOTES

12a. DISTRIBUTION/AVAILABILITY STATEMENT
APPROVED FOR PUBLIC RELEASE: DISTRIBUTION IS UNLIMITED

12b. DISTRIBUTION CODE

13. ABSTRACT *(Maximum 200 words)*

The objective of this work has been to study the interaction between heat release and mixing in compressible shear layers by analysis and computation, with an eye to finding flow configurations that maximize the heat release per unit distance in the stream direction. The principal prediction is that heat release asymmetry across the layer can enhance mixing over the non-heat release case, but the effect appears too small to yield practical benefits at this time. Time-dependent, three-dimensional numerical simulations of a shear layer with weak, steady heat release have shown that such heat release need not decrease mixing, but the expected increases are also absent, or too small to be detected currently. However, the original non-heat-release theory has been successfully extended to predict the mixing behavior of three-dimensional planar layers and round compressible jets. This bolsters confidence in the generality of the principles underlying the analysis. Invoking a mixing maximum principle, the extended theory gives a satisfactory analytic expression for mixing ratio when $M_c \leq 3$. A variational formulation of the heat release problem with a functional dependent on the square of streamline curvature has proved intractable.

14. SUBJECT TERMS	15. NUMBER OF PAGES
Shear Layer, Compressibility, Mixing, Heat Release	36
	16. PRICE CODE

17. SECURITY CLASSIFICATION OF REPORT	18. SECURITY CLASSIFICATION OF THIS PAGE	19. SECURITY CLASSIFICATION OF ABSTRACT	20. LIMITATION OF ABSTRACT
UNCLASSIFIED	UNCLASSIFIED	UNCLASSIFIED	UL

AD-A278328

CONTROLLING COMBUSTION AND MAXIMIZING HEAT RELEASE IN A REACTING COMPRESSIBLE FREE SHEAR LAYER

AFOSR Contract No. F49620-91-C-0020

Principal Investigators: David Nixon, Laurence Keefe

Nielsen Engineering & Research, Inc.
526 Clyde Avenue
Mountain View, CA 94043-2287

ABSTRACT

The objective of this work has been to study the interaction between heat release and mixing in compressible shear layers by analysis and computation, with an eye to finding flow configurations that maximize the heat release per unit distance in the stream direction. The principal prediction is that heat release asymmetry across the layer can enhance mixing over the non-heat release case, but the effect appears too small to yield practical benefits at this time. Time-dependent, three-dimensional numerical simulations of a shear layer with weak, steady heat release have shown that such heat release need not decrease mixing, but the expected increases are also absent, or too small to be detected currently. However, the original non-heat-release theory has been successfully extended to predict the mixing behavior of three-dimensional planar layers and round compressible jets. This bolsters confidence in the generality of the principles underlying the analysis. Invoking a mixing maximum principle, the extended theory gives a satisfactory analytic expression for mixing ratio when $M_c \leq 3$. A variational formulation of the heat release problem with a functional dependent on the square of streamline curvature has proved intractable.

NOMENCLATURE

a_c	=	speed of sound in reference frame of large structures of layer
a_∞	=	speed of sound in the free stream
b	=	parameter in expression for heat release, h_f
c	=	parameter in expression for heat release, h_f
h_f	=	enthalpy due to heat release in the shear layer
$\underline{m}$	=	mixing rate
m	=	non-dimensional mixing rate
m_o	=	reference mixing rate
m_{oi}	=	reference incompressible mixing rate
q_c	=	large structure convection velocity
q_∞	=	reference velocity
s	=	reference surface area for mixing rate determination
t	=	time
u	=	streamwise perturbation velocity due to shear layer = $\phi_x + \psi_y$
v	=	normal perturbation velocity due to shear layer = $\phi_y - \psi_x$
x	=	streamwise coordinate

y = coordinate transverse to the mixing layer
D = parameter in expression for heat release, h_f
C_v = specific heat at constant volume
E_v = perturbation energy
E_s = energy entrained due to mixing
E_o = reference energy
E_∞ = total energy
F = square of the streamline curvature, K^2
H = total (volume integrated) heat release per flow distance
K = streamline curvature
M_c = convective Mach number of large structures in a shear layer
M_∞ = reference Mach number
M_j = jet exit Mach number
RKE = rotational kinetic energy of a vortex
S = streamline arclength
$\overline{T}$ = average layer temperature
T_∞ = reference temperature
U_o = reference velocity
V = entrainment velocity
V = control volume in mixing analysis with no heat release
α = parameter in odd component of heat release, h_f
β^2 = $1-M_\infty^2$, or $1-M_c^2$
γ = specific heat ratio
η = transverse source coordinate in Poisson equation integral solution
η' = $\eta-y$
θ_s = helical angle of a helical jet vortex
ρ = fluid density
ϕ = potential for irrotational part of perturbation velocity
ψ = stream function for solenoidal part of perturbation velocity
ω = vorticity
ξ = streamwise source coordinate in Poisson equation integral solution
Γ = vortex strength

$$\Gamma_o = \gamma M_c^2 \int (\omega/U_c)\, dy$$

INTRODUCTION

A major problem in developing hypersonic aircraft is the design of an efficient propulsion system. One of the most difficult aspects of propulsion design is to get the fuel and air mixed sufficiently so that combustion is maximized inside the engine. At the mass flux rates of fuel and air necessary to produce the design thrust, the fluid streams are moving at high supersonic speeds. As the difference between the stream Mach numbers increases, the mixing of the streams decreases, with a corresponding loss in combustion efficiency. This mixing decrease correlates well with the "convective Mach number," which is essentially a density weighted difference of the Mach numbers of the streams. If the convective Mach number is unity, then experimental results[1] show that the mixing is about

25% of its value at a convective Mach number of zero. There is a considerable body of literature on the causes of this deterioration in mixing, including experimental, computational, and theoretical studies.

Earlier work[2] examined the mixing of supersonic shear layers, both theoretically and computationally, with the conclusion that mixing is inhibited at higher convective Mach numbers (M_c) because energy that would be directly transmitted into mixing at $M_c = 0$ instead goes into nonmixing gas compression. This compressibility effect is largely two-dimensional; introducing three-dimensionality into the flow (streamwise vortices) reduces but does not eliminate it for $M_c > .7$. Comparison of experimental growth rates to the theory in Reference 2 suggests that such changes in flow topology are occurring naturally for high M_c layers, and little else can be done. Without these changes mixing would be even less than is measured.

Dismaying as these results are, it should be borne in mind that the ultimate goal is not just mixing of inert species, but rather mixing of fuel and oxidant for combustion. The heat release associated with combustion can be expected to modify the structure of the shear layer, and this in turn affects its mixing rate. Thus it is appropriate to study the coupling of mixing and heat release, for there may be interactions between them that could lead to more efficient combustion than inert mixing results alone indicate.

There have been a number of experimental studies,[3,4] as well as some numerical work,[5,6] on the effect of heat release on low speed mixing layers ($M_{1,2} < .35$). All studies conclude that heat release decreases the layer growth rate, except for the work of Keller and Daily. This one experiment is distinguished by its use of hot combustion products in one stream to ignite completely premixed fuel/air in the other stream. Other studies assume a symmetric placement of unburnt fuel in one stream, oxidant in the other. Keller and Daly are the only ones to report an increase in mixing layer growth rate with increased heat release. Within the framework of the present analyses such asymmetries are demonstrated to be mixing enhancers.

The previously developed theory[2] for nonreacting shear layers produced an analytical prediction of the reduced mixing observed in experiment. This prediction was made by discarding previous arguments relating reduced mixing to reduced instability[7,8] and employing the insight that this phenomenon is explainable by considering wholly irrotational compressibility effects. In the present work this analysis is extended to include the effects of weak heat release and entropy generation with and without vorticity. The theory is meant to be valid at high speeds ($M_c \sim O(1)$), and this results in somewhat different governing equations than appear in analysis of heat release in flows as $M_c \to 0$.[9] The results indicate that mixing rates can be either increased or decreased by proper tailoring of the heat release profile across the layer.

ELEMENTS OF THE THEORY FOR INERT MIXING

The physical configuration of a compressible free shear layer is shown in Figure 1, where ω_z vorticity contours have been drawn from the results of two-dimensional direct numerical simulations of this flow. Two parallel streams, initially separated by a splitter

plate, and semi-infinite in directions transverse to the mean flow, mix at their interface. The upper stream is characterized by ρ_1, U_1, a_1, and the lower by ρ_2, U_2, a_2 ($U_1 \geq U_2$ assumed). Static pressures in the stream are matched at the trailing edge of the splitter plate so that no expansion/compression waves contaminate the streamwise development of the flow. Initial instability of this shear layer causes it to roll up into spanwise vortices which subsequently pair due to a further spatial subharmonic instability. As the roll-up and growth of vortices proceeds, the width of the shear layer grows downstream, and increasing amounts of fluid are entrained from both sides. The growth rate of incompressible shear layers depends on their velocity and density ratios. High speed shear layers, however, grow much more slowly than their incompressible counterparts at the same velocity and density ratios. Bogdanoff,[1] and later Papamoschou and Roshko,[10] suggested that the effect of compressibility on growth of a shear layer is characterized by Mach numbers M_{c_i} measured relative to the convective speed U_c of the large structures.

Thus

$$M_{C_1} = \frac{U_1 - U_C}{a_1}, \qquad M_{C_2} = \frac{U_C - U_2}{a_2} \tag{1}$$

A relation between M_{c_1} and M_{c_2} is obtained by assuming that the two streams have equal static pressures, and that their stagnation values in the U_c reference frame are also equal. If it is further assumed that the ratio of specific heats γ_i for each stream are equal, then $M_{c_1} = M_{c_2} = M_c$, and the convective velocity may be calculated as a sound speed weighted average

$$U_c = \frac{a_2 U_1 + a_1 U_2}{a_1 + a_2} \tag{2}$$

The dominant feature of a mixing layer at lower values of M_c is the existence of large vortical structures. If these structures are regarded as characteristics of the flow, then an analysis based on the behavior of these structures with increasing convective Mach number should also reflect the behavior of the complete mixing layer with increasing M_c. The theory of Reference 2 has three elements. The first is an expression for the energy within a control volume circumscribing a portion of the turbulent shear layer, in terms of the mixing rate (rate of increase of mass within the volume) and convective Mach number M_c. In the second element the mixing rate of an isolated vortex is shown to be proportional to the square root of its energy, and this establishes a scaling between the mixing rate due to an arbitrary vortex and that of a reference vortex, based on the ratio of their energies. Identifying the energy and mixing rate of the control volume analysis with that of an arbitrary vortex yields a relation between the nondimensionalized mixing in the shear layer and the energy and mixing due to a reference, isolated vortex sitting in a uniform free stream of Mach number M_c. The basic result can be written as

$$\frac{\bar{m}}{\bar{m}_i} = \left[\frac{m_o}{m_{oi}}\right]^2 \left[\frac{(RKE)_{oi}}{(RKE)_o}\right] \tag{3}$$

where $\bar{m}$ denotes non-dimensional mixing of the mixing layer, the subscript i indicates values at M_c=0, and m_o denotes non-dimensional mixing associated with a reference vortex in which the rotational kinetic energy (RKE) is $(RKE)_o$.

Finally, in the third element of the theory the reference vortex is taken to be the bound circulation of a lifting airfoil. Both the mixing and energy of this reference "vortex" can be calculated analytically from solution of the Prandtl-Glauert equation with $M_\infty = M_c$.

$$(1 - M_c^2)\phi_{xx} + \phi_{yy} = 0 \tag{4}$$

The analytic prediction of the theory for the mixing ratio at lower values of M_c ($M_c \leq 0.7$) (ratio of mixing $\bar{m}$ at M_c to mixing at M_c=0, m_i, holding density and velocity ratio constant) is

$$\frac{\bar{m}}{\bar{m}_i} = \frac{(1 - M_c^2)^{3/2}}{1 - \frac{M_c^2}{2}} \tag{5}$$

Plotted as the solid line, the central character of this relation with respect to the experimental scatter for $M_c < .7$ can be seen in Figure 2. A modification to this theory, described in later sections, extends it to greater values of M_c, by allowing for three-dimensionality

The airfoil analogy and its solution by potential methods is a framework that embodies several important physical effects relevant to mixing. Replacement of the shear layer by the velocity difference across the airfoil reduces the mixing problem to the simplest terms: given a horizontal velocity difference (whose integral over the chord is the bound circulation of the airfoil), what is the vertical velocity (downwash, entrainment velocity) that it induces? The answer to this question provided by a potential flow solution to the airfoil problem necessarily implies that the predicted effects are irrotational. The quantitative accuracy of Equation (2) in predicting observed mixing decreases strongly implies that both the instability[7,8] and vorticity redistribution[11] arguments simply miss the point. The physical explanation for the irrotational decrease of mixing is simpler: compressibility directly attenuates the large structures' ability to deflect fluid away from the free streams and into the mixing layer. In incompressible layers "pushing" on the free stream by the entrainment velocity deflects fluid into the layer; in compressible layers "pushing" produces fluid compression also and thus less deflection.

MIXING THEORY WITH HEAT RELEASE AND VORTICITY

The same three elements make up the theory for mixing with heat release as did the theory for mixing without heat. However, the simple scaling relations that lead to Equation (5) can no longer be obtained when heat release is included. Instead, the analysis results in a general expression for the nondimensional mixing that can be made specific by assumption of a particular heat release configuration.

The analysis is best understood in the context of the control volume and vortex model depicted in Figures 3 and 4. The mixing per unit span of the vortex is defined by

$$m = \int_{-x_1}^{x_1} \rho_o |v| dx \tag{6}$$

where now the entrainment or downwash velocity v is assumed to have three components

$$v = v_{pg} + v_h + v_\omega \tag{7}$$

This decomposition looks ahead to the inhomogeneous Prandtl-Glauert equation that will ultimately be solved for v, and which has homogeneous solution v_{pg} and specific solutions v_h and v_ω. Then the mixing can be written

$$m = m_{pg} + m_h + m_\omega \tag{8}$$

where m_h is the mixing due to heat release, m_ω is the mixing due to vorticity, and m_{pg} is the value using the Prandtl-Glauert equation.

Similar to the original analysis,[2] the control volume balance yields

$$\hat{E}_S - \hat{E}_H = C_v \bar{T} m \left(1 + \frac{\gamma(\gamma-1)}{2} M_o^2\right) t \tag{9}$$

where $\hat{E}_H$ is the energy in the mixed region due to heat release and $\hat{E}_S$ is the total energy in the mixed region. One may also write for the isolated vortex

$$\bar{m}_{pg} = \bar{m}_o \frac{(\hat{E}_S - \hat{E}_H)^{1/2}}{\hat{E}_o^{1/2}} \tag{10}$$

where $\hat{E}_o$ and $(\hat{E}_s - E_H)$ are the rotational kinetic energy of the Prandtl-Glauert vortex at the reference condition and the current condition respectively. Using Equation (9) and proceeding as in Reference 2 gives the equation

$$\frac{(\hat{E}_s - \hat{E}_H)}{E_\infty} = \frac{\bar{m}_o}{\bar{E}_o^{1/2}} \frac{(\hat{E}_s - \hat{E}_H)^{1/2}}{E_\infty^{1/2}} + \bar{m}_h + \bar{m}_\omega \tag{11}$$

where E_∞ and $\overline{E_o}$ are given by

$$\bar{E} = \frac{\hat{E}_o}{E_\infty \rho_o V}$$

$$E_\infty = C_v T_\infty \left(1 + \frac{\gamma(\gamma+1)}{2} M_\infty^2 \right)$$

and V is a normalizing volume derived from the control volume balance. See Reference 2 for details.

Equation (11) is quadratic in $\dfrac{\left[\hat{E}_s - \hat{E}_H\right]^{1/2}}{E_\infty^{1/2}}$; thus

$$\frac{(\hat{E}_s - \hat{E}_H)^{1/2}}{E_\infty^{1/2}} = \frac{1}{2} \left\{ \frac{\bar{m}_o}{\bar{E}_o^{1/2}} \pm \left[\frac{\bar{m}_o^2}{\bar{E}_o} + 4\bar{m}_h + 4\bar{m}_\omega \right]^{1/2} \right\} \tag{12}$$

and, hence, from Equations (9) and (11)

$$\bar{m} = \frac{1}{2} \left\{ \frac{\bar{m}_o^2}{\bar{E}_o} \pm \frac{\bar{m}_o}{\bar{E}_o^{1/2}} \left[\frac{\bar{m}_o^2}{\bar{E}_o} + 4m_h + 4\bar{m}_\omega \right]^{1/2} \right\} \tag{13}$$

In order to recover the nonreacting result, the positive sign is taken. If the assumption is made that

$$|\bar{m}_h + \bar{m}_\omega| << \frac{\bar{m}_o^2}{\bar{E}_o} \tag{14}$$

then Equation (14) gives the simple equation

$$\bar{m} = \frac{\bar{m}_o^2}{\bar{E}_o} + 2\bar{m}_s + 2\bar{m}_\omega \tag{15}$$

The inert mixing theory produces just the first term on the right hand side of Equation (15), and this leads immediately to Equation (3).

To proceed further the entrainment velocity v must be solved for. This can be obtained from a Poisson equation for the irrotational part of the velocity field. The analysis leading to this equation is quasi-steady. While molecular mixing within the layer cannot be treated in this manner, the entrainment process by which the layer grows can. In particular note that the temporal rate of change of large structures within the layer is of the order of the spreading rate, and this is small. The steady energy equation for specific enthalpy, h, of fluid in the layer is given by

$$h + (1/2)q^2 = h_o + h_f \tag{16}$$

where h_o is the stagnation enthalpy, h_f is the heat release, and q is the magnitude of the total fluid velocity.

If the inviscid momentum and energy equations are combined, the steady Crocco equation results

$$\nabla(h + \tfrac{1}{2}q^2) = \nabla h_o + \nabla h_f = T\nabla S + \bar{q}x\omega \tag{17}$$

where $\bar{q}$ is the velocity vector, T is temperature, S is entropy, and ω is vorticity. But, h_o is taken to be a constant and thus

$$\nabla h_f = T\nabla S + \bar{q}x\omega \tag{18}$$

In the absence of any other generators of entropy the heat release appears as an increase of entropy and vorticity. Now let the cartesian perturbation velocity components u and v be written as

$$u = \phi_x + \psi_y;\ v = \phi_y - \psi_x \tag{19}$$

where ϕ is the perturbation velocity potential and ψ is the stream function given by

$$\psi_{xx} + \psi_{yy} = -\omega/U_\infty \tag{20}$$

From the energy equation the density, ρ, can be written in terms of the velocity and entropy as

$$\frac{\rho}{\rho_\infty} = \left\{1 + \frac{(\gamma-1)h_f}{a_\infty^2} + \frac{(\gamma-1)}{2} M_\infty^2 \left(1 - \frac{q^2}{U_\infty^2}\right)\right\}^{\frac{1}{\gamma-1}} \exp(-(S-S_\infty)/R) \tag{21}$$

The assumption of weak heat release and small entropy change

$$\frac{(\gamma-1)h_f}{a_\infty^2} \quad , \quad \frac{S - S_\infty}{R} \quad << 1$$

allows this state equation to be linearized. When combined with the continuity equation

$$\nabla\cdot(\rho\bar{q}) = 0 \tag{22}$$

and eliminating second order terms in the perturbations (velocity, heat and entropy), a Poisson equation for the perturbation potential results.

$$(1 - M_\infty^2)\phi_{xx} + \phi_{yy} = \left[\frac{S-S_\infty}{R} - \frac{h_f}{a_\infty^2} \right]_x + M_\infty^2 \psi_{xy} \tag{23}$$

The right hand side of Equation (23) can be simplified by considering the two components of the Crocco equation. At this order

$$\begin{aligned} (h_f)_x &= T_\infty S_x \\ (h_f)_y &= T_\infty S_y - U_\infty \omega \end{aligned} \tag{24}$$

Integrating the first of this pair, differentiating by y and comparing with the second shows that

$$h_f = T_\infty S - \int U_\infty \omega \, dy \tag{25}$$

Then defining

$$\Gamma = \gamma M_\infty^2 \int (\omega/U_\infty) \, dy \tag{26}$$

the governing equations become

$$(1 - M_\infty^2)\phi_{xx} + \phi_{yy} = \frac{(\gamma-1)(h_f)_x}{a_\infty^2} + M_\infty^2 \psi_{xy} + \gamma M_\infty^2 \Gamma_x \tag{27}$$

and Equation (20). The formal solution of the above equation is described in the following section.

SOLUTION FOR THE ENTRAINMENT VELOCITY

The formal solution of the Poisson Equation (27) for the perturbation potential can be found in any text on mathematical physics. It involves integration of the right hand side of Equation (27), multiplied by the appropriate Green's function, over the spatial domain of the problem. In the context of the nonreacting analysis this two-dimensional volume integral was transformed into a line integral over the chord of a thin lifting airfoil whose bound circulation was given by the velocity difference of the two streams of the mixing layer. Here the same approach is taken, with the "source" function on the right hand side of Equation (27) assumed to be confined to the plane y=0. Using the integral equation analysis of Reference 12, a formal solution to Equation (27) can be written as

$$v = v_{pg} + v_h + v_\omega \tag{28}$$

where v_{pg} denotes the value for the Prandtl Glauert equation (Equation (27) with the right hand side equated to zero). v_h and v_ω are given by

$$v_h = \frac{-1}{\pi} \int_0^1 \frac{L(I_{f_1})}{x - \xi} d\xi + I_{f_1}$$

$$v_\omega = \frac{-1}{\pi} \int_0^1 \frac{L(I_{f_2})}{x - \xi} d\xi + I_{f_2} \tag{29}$$

where

L() is the operator on I_f given by

$$L(I_f) = \frac{1}{\pi} \left[\frac{1-x}{x}\right]^{1/2} \int_0^1 \frac{I_f}{x-\xi} \left[\frac{\xi}{1-\xi}\right]^{1/2} d\xi \tag{30}$$

and

$$I_{f_1} = \frac{1}{2\pi} \int\int_{D_1} K_x \{(h_{f_\eta}(\xi,\eta) + h_{f_\eta}(\xi,-\eta))\} d\xi d\eta$$

$$I_{f_2} = \frac{1}{2\pi} \int\int_{D_1} K_x \{(\lambda(\xi,\eta) + \lambda(\xi,-\eta))\} d\xi d\eta \tag{31}$$

The kernel K is the two dimensional Green's function

$$K = \tfrac{1}{2} \ln | (x-\xi)^2 + \eta^2) | \tag{32}$$

for the upper half plane D_1, and

$$\lambda = M_\infty^2(\psi_{yy} - \gamma\omega/U_\infty) \tag{33}$$

The structure of the integrals in Equation (31) makes clear the possibilities for mixing increase or decrease when heat release is present. Specifically, if h_f is even or λ is odd in y, then v_h and v_ω are zero and the mixing is unaffected. On the other hand, if h_f is odd and λ is even then both additional velocities will be non-zero, and mixing can be increased or decreased. v_h can be either positive or negative dependent upon which side of the layer the heat release is concentrated, while the sign of v_ω depends upon a combination of streamline curvature and vorticity whose physical interpretation is difficult to determine.

Some further simplifications of the expressions for entrainment velocity due to heat release can be made if a particular mixing model, the vortex, is assumed. In Equation (29), an airfoil analogy is used and the chord of the airfoil is assumed to be unity. If the dominant flow structure is a simple vortex centered at x_o then this chord approaches zero, or, in the case of the line integral in Equation (29)

$$|x| >> |\xi| \tag{34}$$

Hence

$$I_{f_1}(x) = I_{f_1}(x_o) \tag{35}$$

Also, then

$$-\frac{1}{\pi} \int_0^1 \frac{L(I_{f1})}{x - \xi}\, d\xi \rightarrow \frac{-I_{f1}(x_o)}{\pi} \int_0^1 \left[\frac{1 - \xi}{\xi}\right]^{1/2} \frac{d\xi}{x - \xi} \tag{36}$$

and the velocity v_h is given by

$$v_h = \frac{-I_{f1}(x_o)}{\pi} \int_0^1 \left[\frac{1 - \xi}{\xi}\right]^{1/2} \frac{1}{(x - \xi)}\, d\xi + I_{f1}(x) \tag{37}$$

The mixing rate $\overline{m}_h$ is then given by

$$\bar{m}_h = \rho_o \frac{|I_{f_1}(x_o)|}{\pi} \left\{ \int_0^1 \left[\frac{1-\xi}{\xi}\right]^{1/2} \ln\left|\frac{x_2-\xi}{\xi}\right| d\xi + \int_0^1 \left[\frac{1-\xi}{\xi}\right]^{1/2} \ln\left|\frac{x_1-\xi}{\xi}\right| d\xi \right\} \tag{38}$$

$$+ \left| \int_{x_1}^{x_2} I_{f_1}(x)\,dx \right|$$

I_{f1} can be rewritten, using an integration by parts, as

$$I_{f_1}(x) = \frac{1}{2\pi} \int\int_{D_1} K_{xy} \quad [h_f(\xi,\eta) - h_f(\xi,-\eta)]\,d\xi d\eta \tag{39}$$

NUMERICAL SIMULATIONS WITH STEADY HEAT RELEASE

After addition of an independently specifiable heat release term to the energy equation in our Navier-Stokes simulations, the effect of steady, but spatially varying, heating on a two-dimensional shear layer has been investigated. The heating profile is specified as a shifted Gaussian:

$$h_f(x,y) = D \frac{a_\infty^2}{\gamma-1} \; e^{-\sigma((y-b)/(1+cx))^2} \Big/ (1+cx) \tag{40}$$

By varying D, b, σ and c the intensity, displacement and spreading rate of the heating profile can be adjusted in a parameter study. Because of the particular form chosen the total heat release per unit distance in the flow direction is constant, consistent with linear growth of a reacting shear layer. Previously reported experiment[3] and simulation[5] have left the general impression that heating reduces shear layer growth, although there is one report[4] to the contrary. Although mixing rate increases due to heating asymmetry were not found in the parameter study, neither were decreases in mixing detected. Figures 3 and 4 are typical of the simulation results and display the spreading rates and temperature contours of an M_c=.4 layer with and without heating. Normalized temperature contours ($(T-T_\infty)/T_\infty$) are shown only for the heated layer, since at the same contour resolution the unheated layer has no perceptible variation. The parameter values for the heat release are D=.002, b=1., σ=2. and c=.02. For these conditions the heat is released completely within the layer and the time averaged temperature rise of the fluid within the turbulent part of the flow reaches a centerline peak more than 30% greater than its unheated value. Yet the spreading rate, measured by the vorticity thickness δ_ω, is essentially unaffected. Such cases have not been analyzed in detail, but they indicate, along with the strong heat release cases reported in Reference 4, that there can be heat release scenarios without decreased mixing.

AN ANALYTIC EXAMPLE OF HEAT RELEASE

Prompted by the anomalous results of the simulations an analytic heat release example was solved to better understand the functional dependence of the entrainment velocity upon heat release parameters. The field equation for the perturbation velocity potential due to heat release $h_f(x,y)$ is

$$\phi_{xx} + \phi_{yy} = \frac{\gamma-1}{a_\infty^2 \beta^2} \; h_{f_x}(x,y) \tag{41}$$

The analysis begins with the expression for V, the velocity normal to the layer, gotten from a y-differentiation of the expression for the potential ϕ that solves the governing Poisson equation. This is

$$V(x,y) = \phi_y(x,y) = \frac{(\gamma-1)}{2\pi a_\infty^2 \beta^2} \int_\xi \int_\eta \frac{(y-\eta) h_{f_\xi}}{[\,(x-\xi)^2 + (y-\eta)^2\,]} \, d\eta \, d\xi \tag{42}$$

Note the asymmetry of the kernel in Eq. (42); unless $h_{f\xi}$ has some asymmetry in η with respect to the y-value of the field point, the η integral evaluates to zero. Thus, for a given heat release distribution $h_{f\xi}$, it is only its component odd with respect to y that is important to the entrainment velocity V at y.

For simplicity, assume a separable form for $h_f(\xi,\eta)$

$$h_f(\xi,\eta) = Hf(\xi)g(\eta) \tag{43}$$

where $f(\xi)$, $g(\eta)$, $H > 0$ and $\int\int h_f \, d\eta d\xi$ must be finite.

Then

$$V(x,y) = \frac{(\gamma-1)H}{2\pi a_\infty^2 \beta^2} \int_{\xi=-\infty}^{\infty} f_\xi \int_{\eta=-\infty}^{\infty} \frac{(y-\eta)g(\eta)}{[(x-\xi)^2 + (y-\eta)^2\,]} \, d\eta \, d\xi \tag{44}$$

Now $g(\eta)$ can be decomposed about any y into a sum of odd and even functions $g_o(y-\eta) + g_e(y-\eta)$. Only g_o contributes to the integral, and so Eq. (44) may be rewritten replacing $g(\eta)$ by $g_o(y-\eta)$. To understand the subsequent behavior of V we choose a generic form for $g_o(y-\eta)$ that has properties appropriate for the odd component of a single maximum (in η) heat release profile. It is

$$g_o(y-\eta) = \frac{-2\alpha}{\pi} \frac{b^3(y-\eta)}{\left[1 + b^2(y-\eta)^2\right]^2} \quad (45)$$

This form has been chosen for its integration properties, its structural resemblance to the odd component (about arbitrary y) of the function $g(\eta) = 1/(1+b^2\eta^2)$, and for its property that as $b\to\infty$, $g_o(y-\eta) \to -\alpha\delta'(y-\eta)$. The constant α controls the sign of the contribution of the heat release above and below y. Substituting Eq. (45) into Eq. (44) yields

$$V(x,y) = \frac{-\alpha b^3(\gamma-1)H}{\pi^2 a_\infty^2 \beta^2} \int_{\xi=-\infty}^{\infty} \int_{\eta=-\infty}^{\infty} \frac{(y-\eta)^2}{\left[(x-\xi)^2+(y-\eta)^2\right]\left[1 + b^2(y-\eta)^2\right]} \, d\eta \, d\xi \quad (46)$$

After a change of variable to $z = y-\eta$, and splitting the integrand into factors, the inner integral can be evaluated to yield

$$V(x,y) = \frac{\alpha b^2(\gamma-1)H}{2\pi a_\infty^2 \beta^2} \int_{\xi=-\infty}^{\infty} \frac{f_\xi}{\left[b(x-\xi)+1\right]^2} \, d\xi \quad (47)$$

For $f_\xi > 0$, i.e., heat release increasing in the streamwise direction, the direction of the entrainment velocity is controlled by the sign of α. This in turn characterizes whether the odd component of the heat release, at a given y, is negative above or below y. In either case, the entrainment velocity goes from the positive portion of the odd component towards the negative. This situation is depicted in Figure 5.

What is the general shape of g_o for a single maximum heat release profile? One can construct the answer graphically, but for

$$g(\eta) = \frac{1}{1 + \eta^2}$$

it can be demonstrated that for $\eta' = \eta - y$

$$g_o(\eta' + y) = \frac{-2\eta' y}{\left[1 + (\eta' + y)^2\right]\left[1 + (-\eta' + y)^2\right]} \quad (48)$$

Thus, for positive y, the negative component of g_o is above y, and the entrainment velocity V is in that direction, away from the heat release. For $y < 0$ the negative portion is below y, and once again the entrainment velocity is away from the heat release. Thus, for increasing

heat release downstream, $f_\xi > 0$, entrainment is decreased, but for $f_\xi < 0$, decreasing heat release downstream, entrainment is increased by heat release.

The problem with the numerical simulations now becomes clearer. Despite the fact that the assumed form of the heat release, Eq. (40), is not separable, the streamwise derivative (f_ξ) can be calculated, and is found to vary in sign with both x and y. However, it appears to be uniformly negative for regions nearby the shear layer, which means the entrainment velocities are towards the mixing. The magnitude of V expected in the simulations can be estimated from the analysis if one identifies $Da_\infty^2/(\gamma-1)$ in Eq. (40) with H in Eq. (43), $\sigma^{1/2}$ with b in Eq. (45), and realizes from x-differentiation of Eq. (40) that

$$h_{f_x} \sim - \frac{1}{(1 + cx)^2}$$

is the maximum value of the streamwise derivative for field points y on the edges of the layer. Thus, $h_{fx} \sim [-1, -.03]$ over the length of the layer and we estimate

$$V \sim - \frac{\sigma (\gamma-1)}{2 \pi a_\infty^2 \beta^2} \frac{Da_\infty^2}{(\gamma-1)}$$

$$\sim - \frac{\sigma D}{2\pi\beta^2}$$

$$\sim - \frac{(2)(.002)}{2\pi(.84)}$$

$$\sim - .00076 \qquad (49)$$

The heat release distribution induces entrainment velocities one to two orders of magnitude smaller than the typical turbulent values of V' in the shear layer. Such effects, though real, could easily be indistinguishable.

EXTENSIONS TO INERT MIXING THEORY

Despite the apparent smallness of the heat release induced entrainment velocities, the effects are believed to tbe real. The broad validity of the principles underlying the analysis can be demonstrated by extending the inert mixing theory to three-dimensions and comparing the predictions with experimental data. The way in which three-dimensional effects can be incorporated in the theory for planer layers and circular jets is described in the following paragraphs.

PLANAR SHEAR LAYERS

The theory developed in Ref. 2 is based on two main arguments: first that the energy into an element of the mixing layer, ABCD in Figure 6, is conserved; secondly, that a percentage (100% in two dimensions) of this energy is converted into rotational energy

associated with the dominant mixing mechanism, which is assumed to be a two-dimensional vortex. This vortex is represented by the potential bound vortex associated with a lifting wing and leads to a simple analytic result if the potential vortex can be represented by the two-dimensional Prandtl Glauert equation

$$\beta^2 \phi_{xx} + \phi_{yy} = 0 \tag{50}$$

where ϕ is a perturbation velocity potential and

$$\beta^2 = 1 - M_c^2 \tag{51}$$

The basic equations derived in Ref. 2 for the nondimensionalized mixing rate, $\bar{m}$, defined by

$$\bar{m} = m/\rho_o U_o s \tag{52}$$

where ρ_o, U_o are the reference values of density and velocity respectively associated with M_c, and m is the mixing role through a surface area s, are as follows: the energy entrained in time t, $\hat{E}_s$, is given by

$$\hat{E}_s = C_v \bar{T} \bar{m} [1 + \tfrac{\gamma(\gamma-1)}{2} M_c^2] \rho_o U_o s t \tag{53}$$

where C_v is the specific heat at constant volume, and $\bar{T}$ is the average temperature in the mixing layer; this is Eq. (9) of Ref. 2 with the nondimensionalized mixing rate, $\bar{m}$, and instead of m the energy of the vortex $\hat{E}$ is given by Eq. (13) of Ref. 2, which is

$$\bar{m} = \bar{m}_o \left[\frac{\hat{E}_v}{\hat{E}_o}\right]^{1/2} \tag{54}$$

where the subscript "o" denotes a known reference state. Provided M is such that

$$M^2 << 2/(\gamma - 1) \tag{55}$$

it is shown in Ref. 2 that over the control volume V,

$$\hat{E}_v = \int_V \left[\frac{(\gamma-1)}{2\gamma}\right] \Delta q^2 \, dV \tag{56}$$

and

$$\hat{E}_\infty = \int_V \frac{(\gamma-1)}{2\gamma} q_\infty^2 dv \simeq \int_V C_v T_\infty \left[1 + \frac{\gamma(\gamma-1)}{2} M_\infty^2\right] dV \tag{57}$$

where M in Eq. (55) is the oncoming Mach number of a two-dimensional vortex and Δq^2 in Eq. (56) is the square of the perturbation velocity due to the vortex, superimposed as a freestream of energy, E_∞ and a velocity U_∞. Eq. (53), (54), (56), and (57) are general relations and are not restricted to two dimensions. In the two-dimensional theory it is assumed that the energy of the vortex, $\hat{E}_v$, is equal to the entrained energy $\hat{E}_s$. If the vortex is inclined to the oncoming stream, as sketched in Figure 7, then not all of the entrained energy is converted into mixing since there will now be an energy flux in the "spanwise" direction through the mixing layer. Hence

$$\hat{E}_V = \eta \hat{E}_s \tag{58}$$

where η represents the fraction of entrained energy transformed into rotational energy. Combining Eq. (53), (54), and (58) and solving for m gives

$$\bar{m} = \eta \frac{\bar{m}_o^2}{\hat{E}_o} C_v \bar{T}\left[1 + \frac{\gamma(\gamma-1)}{2} M_c^2\right](\rho_o U_o st) \tag{59}$$

As in Ref. 2 $\hat{E}_o$ is nondimensionalized by $\hat{E}_\infty \rho_o V$, where

$$\hat{E}_\infty = C_v T_\infty \left[+ \frac{\gamma(\gamma-1)}{2} M_\infty^2\right] \tag{60}$$

to give

$$\hat{E}_o = \bar{E}_o (E_\infty \rho_o V)$$

where V is the slowly growing control volume ABCD in Figure 6. If U_os in Eq. (59) is chosen such that

$$U_o st = V \tag{61}$$

Then Eq. (59) gives

$$\bar{m} = \eta \frac{\bar{m}_o^2}{\bar{E}_o} \left\{ \frac{C_v \bar{T}\left[1 + \gamma\left[\frac{\gamma-1}{2}\right] M_c^2\right]}{C_v T_\infty \left[1 + \frac{\gamma(\gamma-1)}{2} M_\infty^2\right]} \right\} \tag{62}$$

The vortex model is the flow over a two-dimensional vortex by a freestream normal to the vortex. In the frame of reference moving with the vortex, the mixed layer has a temperature of $\bar{T}$ and the oncoming normal flow has a Mach number of $M_c \cos\theta$ (see Figure 7). Consequently, the reference values, T_∞ and M_∞ are chosen to be as follows:

$$\left.\begin{aligned} T_\infty &= \bar{T} \\ M_\infty &= M_c \cos\theta \end{aligned}\right\} \tag{63}$$

$$q_\infty = q_c \cos\theta \qquad]$$

where q_c is the convective velocity of the mixing layer and Eq. (29) now becomes

$$\bar{m} = \eta \frac{\bar{m}_o^{-2}}{\bar{E}_o} \frac{\left[1 + \frac{\gamma(\gamma-1)}{2} M_c^2\right]}{\left[1 + \frac{\gamma(\gamma-1)}{2} M_c^2 \cos^2\theta\right]} \tag{64}$$

It now remains to estimate the conversion factor, η. If

$$M_c^2 << 2/\gamma\text{-}1$$

then, to a first approximation (see Eq. (57))

$$\hat{E}_s \approx \frac{(\gamma-1)}{2\gamma} q_c^2 \tag{65}$$

and consequently

$$\eta = \hat{E}_v / \hat{E}_s = \cos^2\theta \tag{66}$$

Hence the final result is

$$\bar{m} = \frac{\bar{m}_o^{-2}}{\bar{E}_o} \frac{\left[1 + \frac{\gamma(\gamma-1)}{2} M_c^2\right] \cos^2\theta}{\left[1 + \frac{\gamma(\gamma-1)}{2} M_c^2 \cos^2\theta\right]} \tag{67}$$

From Eq. (56) and (57)

$$\bar{E}_o = \int_{\bar{V}} \left[\frac{\gamma-1}{2\gamma}\right] \Delta\bar{q}^{-2} d\bar{V} \tag{68}$$

where $\Delta\bar{q}$ is the nondimensionalized (by q_∞) velocity perturbation due to the vortex and $\bar{V}$ is the nondimensional volume V. Hence,

$$\bar{E}_o = \left[\frac{\gamma-1}{\gamma}\right] \text{RKE} \tag{69}$$

where RKE is the nondimensionalized rotational kinetic energy of the vortex. The mixing can therefore be found in terms of the reference mixing m_o and the reference RKE, $(RKE)_o$. If the mixing is divided by its value at $M_c = 0$, denoted by the subscript i (the usual method of presenting mixing results), then

$$\frac{\bar{m}}{\bar{m}_i} = \left\{\frac{\bar{m}_o^{-2}}{\bar{m}_o^{-2}} \frac{(RKE)_{oi}}{(RKE)_o}\right\}\left\{\frac{\left[1 + \frac{\gamma(\gamma-1)}{2}M_c^2\right]\cos^2\theta}{\left[1 + \frac{\gamma(\gamma-1)}{2}M_c^2\cos^2\theta\right]}\right\} \tag{70}$$

The first term in braces is the result found for two-dimensional vortices in Ref. 2, and by using the Prandtl-Glauert equation, Eq. (50), it was shown that

$$\frac{\bar{m}_o^{-2}}{\bar{m}_{oi}^{-2}} \frac{(RKE)_{oi}}{(RKE)_o} = \frac{\left[1 - M_\infty^2\right]^{3/2}}{1 - M_{\infty/2}^2} \tag{71}$$

Using the definition of M_∞ from Eq. (63) then

$$\frac{\bar{m}}{\bar{m}_i} = \left\{\frac{\left[1 - M_c^2\cos^2\theta\right]^{3/2}}{\left[1 - \frac{M_c^2\cos^2\theta}{2}\right]}\right\}\left\{\frac{\left[1 + \frac{\gamma(\gamma-1)}{2}M_c^2\right]\cos^2\theta}{\left[1 + \frac{\gamma(\gamma-1)}{2}M_c^2\cos^2\theta\right]}\right\} \tag{72}$$

Eq. (72) represents the mixing rate variation with M_c and the unknown sweep angle, θ. It remains now to determine the sweep angle.

Simple differentiation of Eq. (72) shows that there are mixing maximum points when

$$\frac{\partial\left[\frac{\bar{m}}{\bar{m}_i}\right]}{\partial\theta} = 0$$

It is suggested that these maximum points are the only situations that can exist in practice. They occur, for $\gamma = 1.4$, at

$$\left.\begin{array}{l}\theta = 0 \\ M_c\cos\theta = \begin{cases}0.662 \\ 1.777\end{cases}\end{array}\right\} \tag{73}$$

For $M_c < .662$ only the unswept vortex is in equilibrium. If $M_c \geq .662$, the vortex angle, θ, for maximum mixing is given by

$$\cos\theta = .662/M_c \tag{74}$$

which gives two values of θ, namely

$$\theta = \pm\left|\cos^{-1}(.662/M_c)\right| \tag{75}$$

The third possibility, $M_c \cos\theta = 1.777$, is not of present interest since the lowest possible value of M_c that satisfies this relation ($M_c = 1.777$) does not remotely satisfy Eq. (55). The variation of $\bar{m}/\bar{m}_1$ with θ for various Mach numbers is shown in Figure 8.

The question now arises as to when the swept modes actually appear in an experiment. It is plausible to argue that a smooth transition from the unswept to the swept mode will only occur when the mixing rate is the same for both modes, since this would not involve a discontinuous energy entrainment. Consequently, it is suggested that until a value of $M_c = M_c^*$, only the unswept mode is apparent, where M_c^* is the value for which

$$\left[\frac{\bar{m}}{\bar{m}_1}\right]_{\text{unswept}} = \left[\frac{\bar{m}}{\bar{m}_1}\right]_{\text{swept}} \tag{76}$$

and

$$\left[\frac{\bar{m}}{\bar{m}_1}\right]_{\text{swept}} \quad \text{is the maximum value}$$

given by (for $\gamma = 1.4$)

$$\left[\frac{\bar{m}}{\bar{m}_1}\right]_{\text{swept}} = \frac{.21047}{M_c^2} + .05893 \tag{77}$$

Eq. (76) is satisfied when

$$M_c^* = .662$$

Eq. (77) is shown as the dashed curve in Figure 2. The combined two-dimensional and swept vortex analysis agree qualitatively with observed mixing decreases over a wide range of M_c. Its quantitative predictions of mixing decrease run right through the center of the data scatter almost until $M_c = 1$, after which the theory seems to slightly underpredict the observed rates. Note that the swept vortex analysis predicts a finite mixing rate for large M_c and that this rate should be reached by $M_c = 3$. Thus, the invocation of a "mixing maximum" principle within the context of previously described energy considerations accounts qualitatively and, to a large extent, quantitatively for observed mixing decreases. The theory implies that the flattening of mixing rates for $M_c > .66$ should be associated with the appearance of swept or symmetrically swept ribbed structures in the flow.

ROUND JETS

Once again the mixing is assumed dominated by vortices. There are two types of observed vortical structures in the round jet, namely axisymmetric and helical vortices. In both cases the mixing is given by the integral

$$\bar{m} = \rho \int_{-l}^{l} v_r dx \tag{78}$$

where v_r is the radial velocity, x is the axial direction and $2l$ denotes a characteristic length between vortical structures, as shown in Figure 9.

Axisymmetric Vortices

The velocity induced by an axisymmetric vortex ring, with radius r_o is governed by the Prandtl-Glauert equation

$$\beta^2 \phi_{xx} + \phi_{rr} + \frac{1}{r}\phi_r + \frac{1}{r^2}\phi_{\theta\theta} = 0 \tag{79}$$

where θ is the azimuthal angle, ϕ is the perturbation velocity potential, M_c is the convective Mach number, and

$$\beta^2 = 1 - M_c^2 \tag{80}$$

For axisymmetric structures the azimuthal variation is zero. Using Eq. (79) for a ring vortex gives the following formulae for the axial induced velocity, v_x, and the radial induced velocity, v_r.

$$V_x = \frac{\Gamma}{4\pi r_o \beta} \int_o^{2\pi} \frac{[1 - r\cos(\theta-\theta')]d\theta'}{\left[\frac{x^2}{\beta^2} + r^2 + 1 - 2r\cos(\theta-\theta')\right]^{3/2}} \tag{81}$$

$$V_r = \frac{-\Gamma}{4\pi r_o \beta} \int_o^{2\pi} \frac{x\cos(\theta-\theta'))d\theta'}{\left[\frac{x^2}{\beta^2} + r^2 + 1 - 2r\cos(\theta-\theta')\right]^{3/2}} \tag{82}$$

where Γ is the strength of the vortex and r is the radius nondimensionalized by r_o.

Helical Vortices

The effective Mach number is normal to the vortex and hence if the angle of the helix is θ_s the effective Mach number is $M_c \cos\theta_s$ and therefore

$$\beta^2 = 1 - M_c^2\cos^2\theta_s \tag{83}$$

The induced velocities given by one rotation of the helix ($\theta \to 0, 2\pi$) are as follows:

$$V_x = \frac{\Gamma(1+\mu^2)^{1/2}}{4\pi r_o}\int_o^{2\pi} \frac{[1 - r\cos(\theta-\theta')]d\theta'}{\left[\frac{(x-\theta'\mu)^2}{\beta^2} + r^2 + 1 - 2r\cos(\theta-\theta')\right]^{3/2}} \quad (84)$$

$$V_r = \frac{-\Gamma(1+\mu^2)^{1/2}}{4\pi r_o}\int_o^{2\pi} \frac{[(x-\mu\theta')\cos(\theta-\theta')/\beta + \mu\sin(\theta'-\theta)]d\theta'}{\left[\frac{(x-\theta'\mu)^2}{\beta^2} + r^2 + 1 - 2r\cos(\theta-\theta')\right]^{3/2}} \quad (85)$$

$$V_\theta = \frac{\Gamma(1+\mu^2)^{1/2}}{4\pi r_o}\int_o^{2\pi} \frac{[-(x-\mu\theta')\sin(\theta-\theta')/\beta - \mu r + \mu\cos(\theta'-\theta)]d\theta'}{\left[\frac{(x-\theta'\mu)^2}{\beta^2} + r^2 + 1 - 2r\cos(\theta-\theta')\right]^{3/2}} \quad (86)$$

where v_θ is the azimuthal velocity and

$$\mu = \tan\theta_s \quad (87)$$

In the analysis above the angle of the helix is unknown, but fortunately some experimental data is available from the acoustics studies reported by Seiner.[13] The data makes clear that several wavelengths or modes can exist simultaneously at certain values of M_j. The jet Mach number, M_j, can be crudely related to the convective Mach number M_c by

$$M_j = 2M_c \quad (88)$$

and the helical angle, θ_s, can be related to the wave length by

$$\mu = \tan\theta_s \approx \frac{\lambda}{2\pi r_o} \quad (89)$$

where λ is the wavelength. Seiner reports that above a jet Mach number of 1.2 the vortical structures are helical. It is assumed that the dominant source of noise is the vortices passing a point in space.

The variation of μ with M_c can be found from a simple linear fit to the data in Ref. 13 and by using Equations (88) and (89). Thus

$$\mu = \begin{cases} \frac{1}{\pi}(1 + 4.4M_c) \text{ "low mode"} \\ \frac{1}{\pi}(1.5 + 5.5M_c) \text{ "intermediate mode"} \\ \frac{1}{\pi}(1.75 + 6.2M_c) \text{ "high mode"} \end{cases} \quad (90)$$

One of the most interesting features of these angles is that

$$\beta^2\Big|_{max} = \left[\frac{\pi}{4.4}\right]^2 = 0.51 \qquad (91)$$

This implies that the Mach number normal to the vortical structure, $M_c\cos\theta_s$ is less than 0.71. In other words, the oncoming flow is subsonic. In the two-dimensional studies reported in Reference 2 shock waves occurred for Mach numbers above 0.78, implying that for the round jet the structure switches from axisymmetric vortices to helical vortices to avoid shock waves, a hypothesis first advanced in Ref. 2.

Mixing Calculation

The formulae for the velocities given above can now be used to compute the mixing ratio given by Eq. (3). In these calculations the effect of a large number of axisymmetric vortices or a large number of turns of the helical vortices are represented. There is a problem with scaling the mixing rate, because the value of the incompressible mixing is not clear from the Schadow et al[14] data. Consequently, for comparison purposes, the following assumptions are made.

(a) For $M_c < 0.6$ axisymmetric vortices are assumed to exist and the scaling of the mixing is fixed to agree with Schadow et al[14] data at $M_c = 0.26$.

(b) For $M_c > 0.6$ helical vortices are assumed to exist. This figure is obtained from information given by Seiner.[13] The scaling is fixed to match the data at $M_c = 0.6$.

Results from the computations are shown in Figure 10 and it may be seen that theory agrees surprisingly well with the data. Also shown are two curves computed using the high and low modes for the helical vortices: these are not tied to any experimental data points and are scaled by the value a helical vortex model would give at $M_c = 0.0$. It can be seen that mode switching produces little change in the mixing. The most promising avenue to increase mixing is to switch from an axisymmetric structure to a helical structure at as low a Mach number as possible.

VARIATIONAL APPROACH TO HEAT RELEASE MAXIMIZATION

The desire is to maximize the volumetric heat release H

$$H = \int_{x=x_o}^{x_o+L} \int_{y=-\infty}^{\infty} h_f(\phi, \phi_x, \phi_y, \phi_{xx}, \phi_{xy}\ldots?)\,dy\,dx \qquad (92)$$

subject to the constraint that the velocity field satisfy Eq. (41). The key here is to find plausible models to link the specific heat release h_f to the local velocity field (ϕ, ϕ_x, ϕ_y...). Functionals have been defined dependent upon streamline length and/or some positive definite function of the streamline curvature. These two quantities provide a

characterization of the length and wrinkledness of interfaces between reactants, and the expectation was that the longer and more convoluted this interface, the greater the total product formation and heat release. The variational problem involves finding a flow configuration that balances streamline convolution against the diffusive or averaging character of the potential flow constraint.

The first problem to be dealt with is the description of the streamline length and curvature in terms of the potential ϕ. By writing the formal expressions for arclength and curvature of the streamfunction $\psi(x,y)$ in terms of u and v and then substituting the appropriate expressions in terms of the potential ϕ, one obtains the length element as

$$S = \left[1 + \left(\phi_y / \phi_x \right)^2 \right]^{1/2} \tag{93}$$

and the curvature K as

$$K = \frac{\phi_{xy} / \phi_x \left[1 - \left(\phi_y / \phi_x \right)^2 \right]}{\left[1 + \left(\phi_y / \phi_x \right)^2 \right]^{3/2}} \tag{94}$$

Since the streamline length is a positive definite quantity a possible relation between it and heat release can be plausibly assumed. The curvature, on the other hand, may be negative, and thus the heat release can be connected to it only through some positive valued function of K. The magnitude of K is an obvious choice, but leads to analytical difficulties in obtaining the appropriate Euler equation for the variational problem. Instead, it has been assumed $h_f - K^2 = F$. The Euler equation for this functional is

$$- \frac{\partial}{\partial x} F_{\phi_x} - \frac{\partial}{\partial y} F_{\phi_y} + \frac{\partial^2}{\partial x \partial y} F_{\phi_{xy}} = 0 \tag{95}$$

Expanding the x- and y- partial derivatives gives

$$\begin{aligned} &-\phi_{xx} F_{\phi_x \phi_x} - 2\phi_{xy} F_{\phi_x \phi_y} - \phi_{yy} F_{\phi_y \phi_y} + \phi_{xx} \phi_{xy} F_{\phi_x \phi_x \phi_{xy}} + \\ &\left[\phi_{xx} \phi_{yy} + \phi_{xy}^2 \right] F_{\phi_x \phi_y \phi_{xy}} + \phi_{xy} \phi_{yy} F_{\phi_y \phi_y \phi_{xy}} + \phi_{xxyy} F_{\phi_{xy} \phi_{xy}} \\ &+ \left[\phi_{xy} \phi_{xxy} + \phi_{xx} \phi_{xyy} \right] F_{\phi_x \phi_{xy} \phi_{xy}} + \phi_{xxy} \phi_{xyy} F_{\phi_{xy} \phi_{xy} \phi_{xy}} + \\ &\left[\phi_{xy} \phi_{xyy} + \phi_{yy} \phi_{xxy} \right] F_{\phi_y \phi_{xy} \phi_{xy}} = 0. \end{aligned} \tag{96}$$

Realizing that all of the partial derivatives of F with respect to ϕ_x, ϕ_y and ϕ_{xy} are rational functions of these arguments, it is quickly clear that the resulting equation for ϕ is high order and strongly nonlinear(6^{th} order polynomials in ϕ_x, etc.). No obvious simplifications have been found to make the equation analytically tractable, and the strong nonlinearity urges caution in numerical treatment.

WRITTEN PUBLICATIONS

Nixon, D and Keefe, L. R., "The Effect of Heat Release on a Compressible Free Shear Layer," AIAA 92-0181, 1992.

PROFESSIONAL PERSONNEL

Dr. David Nixon
Dr. Laurence R. Keefe

INTERACTIONS

Discussed acoustic implications of jet mixing theory with J. M. Seiner, NASA Langley Research Center, October 2, 1991. Also with Steve Walker and Ken Wurtzler, Wright Labs, Dayton, OH, October 3, 1991.

DISCOVERIES

No new discoveries or patents have resulted from this work.

REFERENCES

1. Bogdanoff, D. W., "Compressibility in Turbulent Shear Layers," AIAA Journal 21, 1983, p926.
2. Nixon, D., Keefe, L., and Kuhn, G., "The Effects of Compressibility on a Supersonic Mixing Layer," AIAA 90-0706, January 1990.
3. Hermanson, J.C. and Dimotakis, P.E., "Effects of Heat Release in a Turbulent, Reacting Shear Layer," Journal of Fluid Mechanics 199, 1989, p333.
4. Keller, J.O. and Daily, J.W., "The Effects of Highly Exothermic Chemical Reaction on a Two-dimensional Mixing Layer," AIAA Journal 23, 1985, p1937.
5. McMurty, P.A., Riley, J.J. and Metcalfe, R.W., "Effects of Heat Release on the Large Scale Structure in Turbulent Mixing Layers," Journal of Fluid Mechanics 199, 1989, p297.
6. Grinstein, F.F. and Kailasanath, K., "Effects of Chemical Energy Release on the Dynamics of Transitional Free Shear Flows," AIAA 90-1452, 1990.
7. Sandham, N. and Reynolds, W. C., "The Compressible Mixing Layer: Linear Theory and Direct Simulation," AIAA 89-0371, 1989.
8. Ragab, S. A. and Wu, J. L., "Linear Instabilities in Two-Dimensional Compressible Mixing Layers," Physics of Fluids A 1, 1989, p957.
9. Moore, D.W. and Pullin, D.I., "The Effect of Heat Addition on Slightly Compressible Flow: The Example of Vortex Pair Motion," Physics of Fluids A 3, 1991, p1907.

10. Papamoschou, D. and Roshko, A., "The Compressible Turbulent Shear Layer: An Experimental Study," Journal of Fluid Mechanics 197, 1988, p453.
11. Lele, S., " Direct Numerical Simulation of Compressible Free Shear Flows," AIAA 89-0374, 1989.
12. Nixon, D., "Calculation of Transonic Flows Using Integral Equation Methods," Ph.D. Thesis, University of London, England, 1976.
13. Seiner, J. M., "Advances in High Speed Aeroacoustics," AIAA 84-2275, 1984.
14. Schadow, K. C., Gutmark, E., and Wilson, K. J.,"Compressible Spreading Rates of Supersonic Coaxial Jets," Experiments in Fluids 10(2/3), 1990, p161.

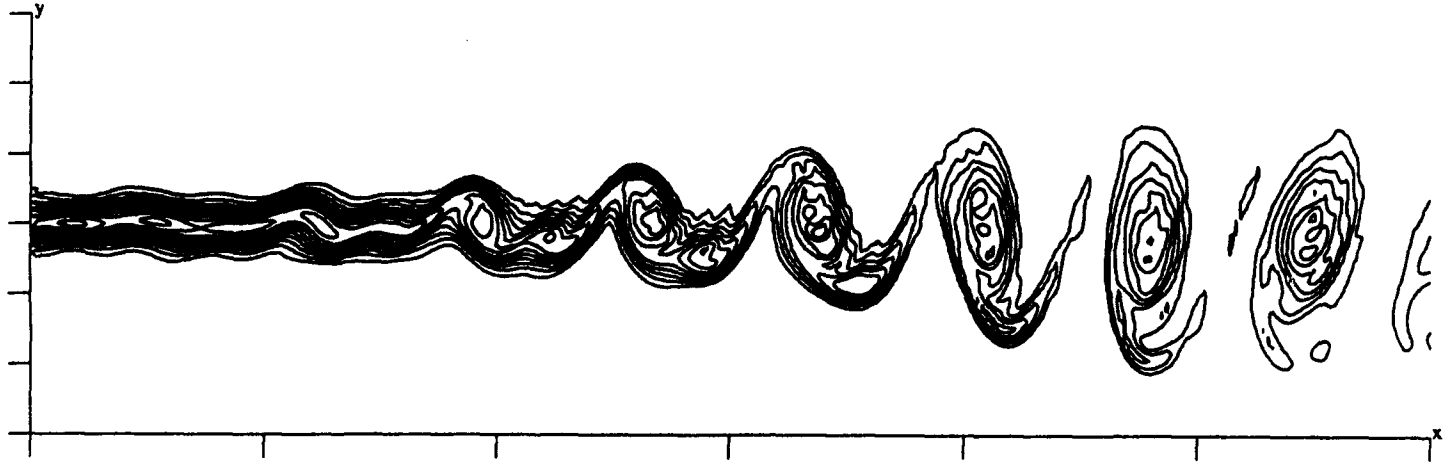

Figure 1. Vorticity contours in a two-dimensional mixing layer, $M_1 = 2.0$, $M_2 = 1.2$, $M_c = .4$

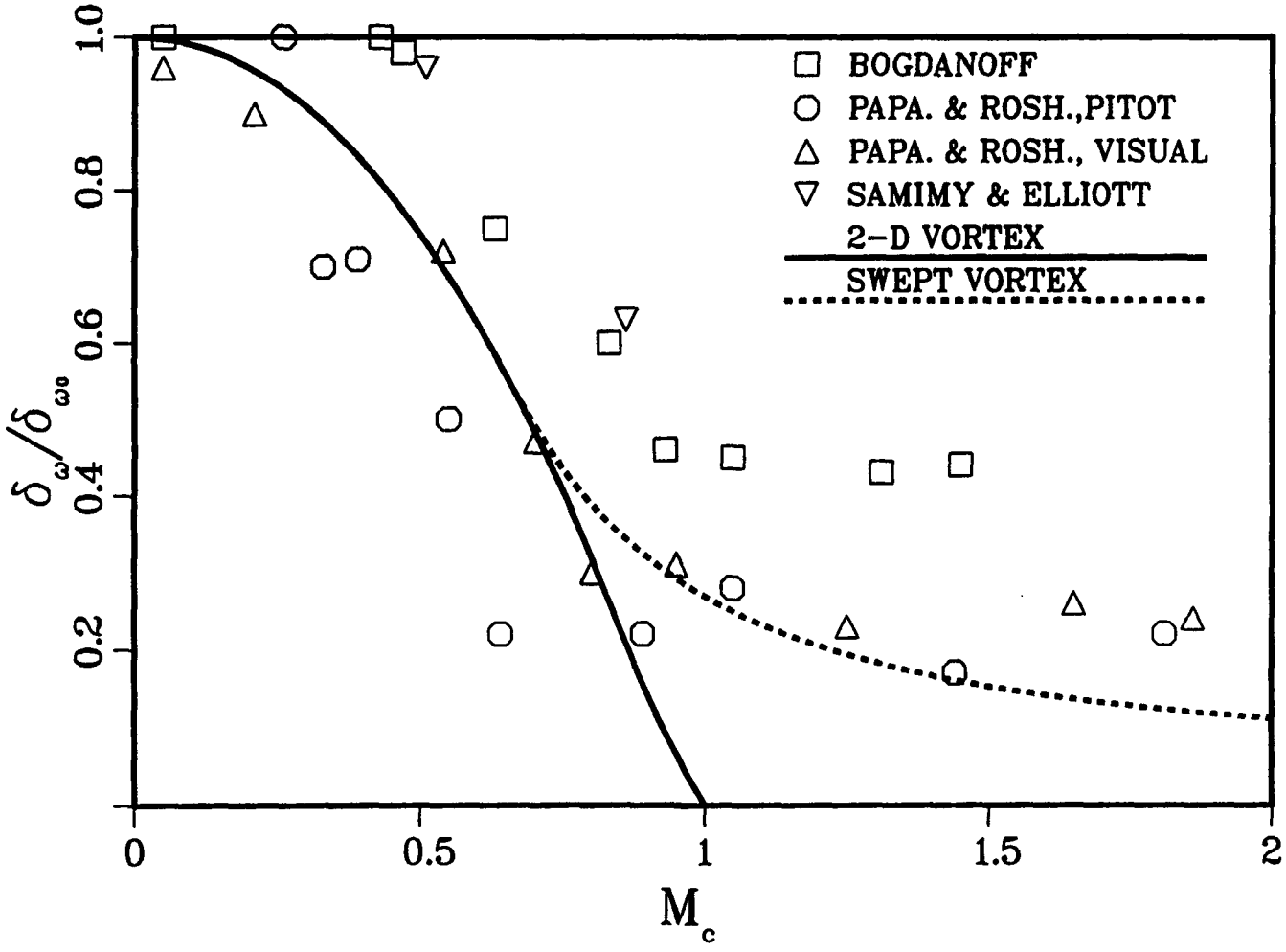

Figure 2. Experimentally measured layer growth rates compared to two-and three-dimensional theory.

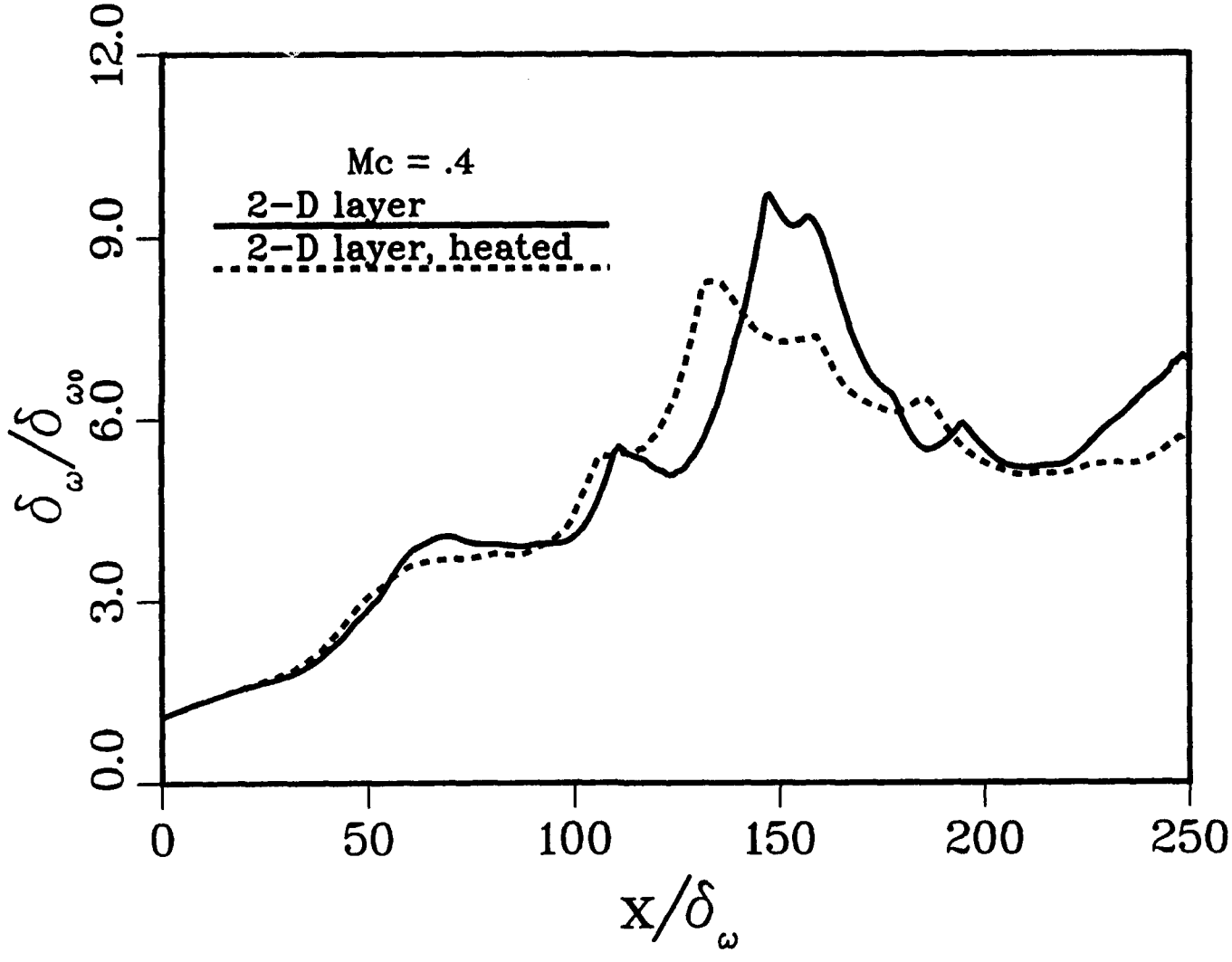

Figure 3. Spreading rates for unheated and heated two-dimensional shear layers, $M_c = .4$

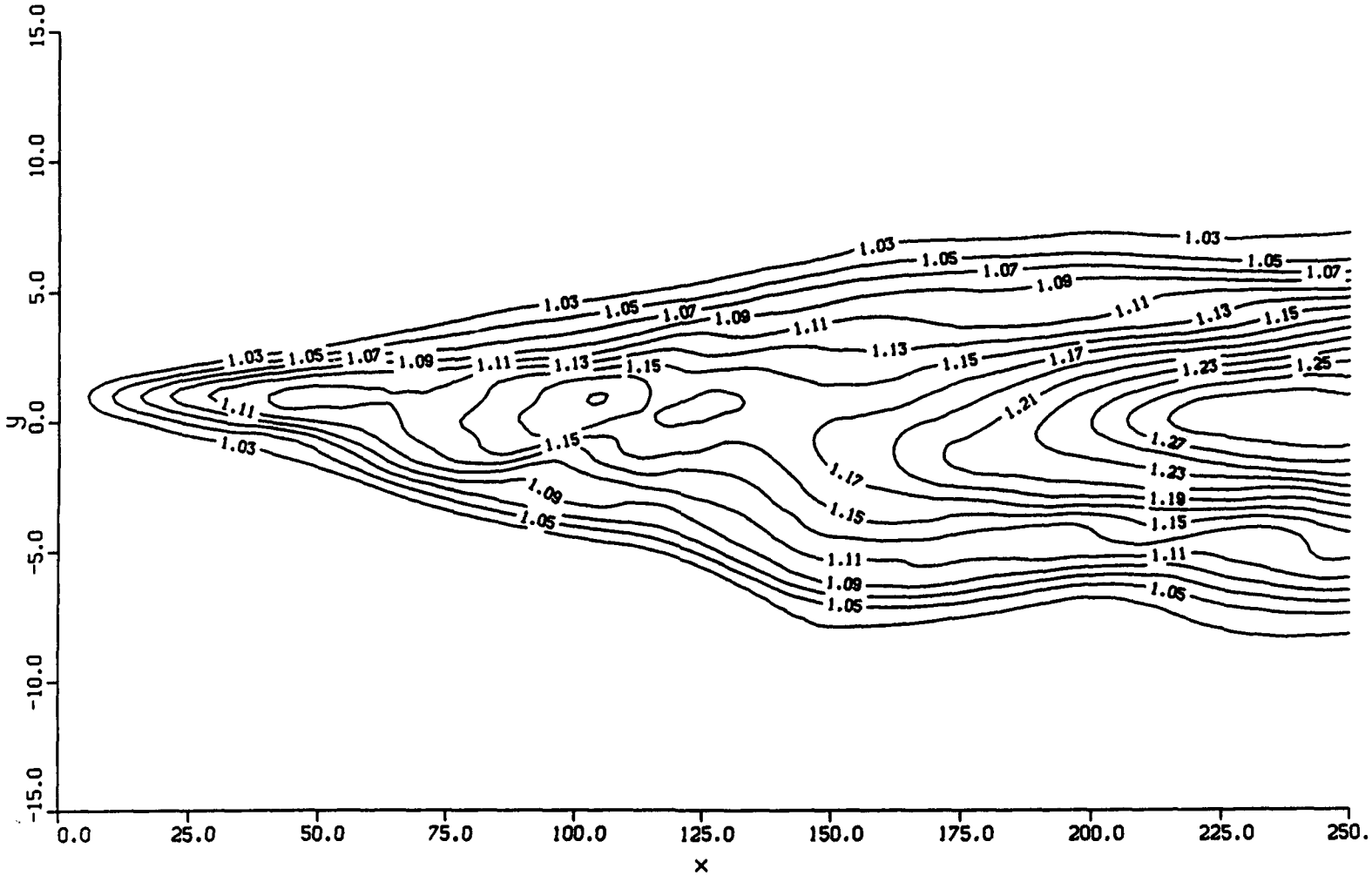

Figure 4. Normalized temperature contours in the heated two-dimensional shear layer, $M_c = .4$

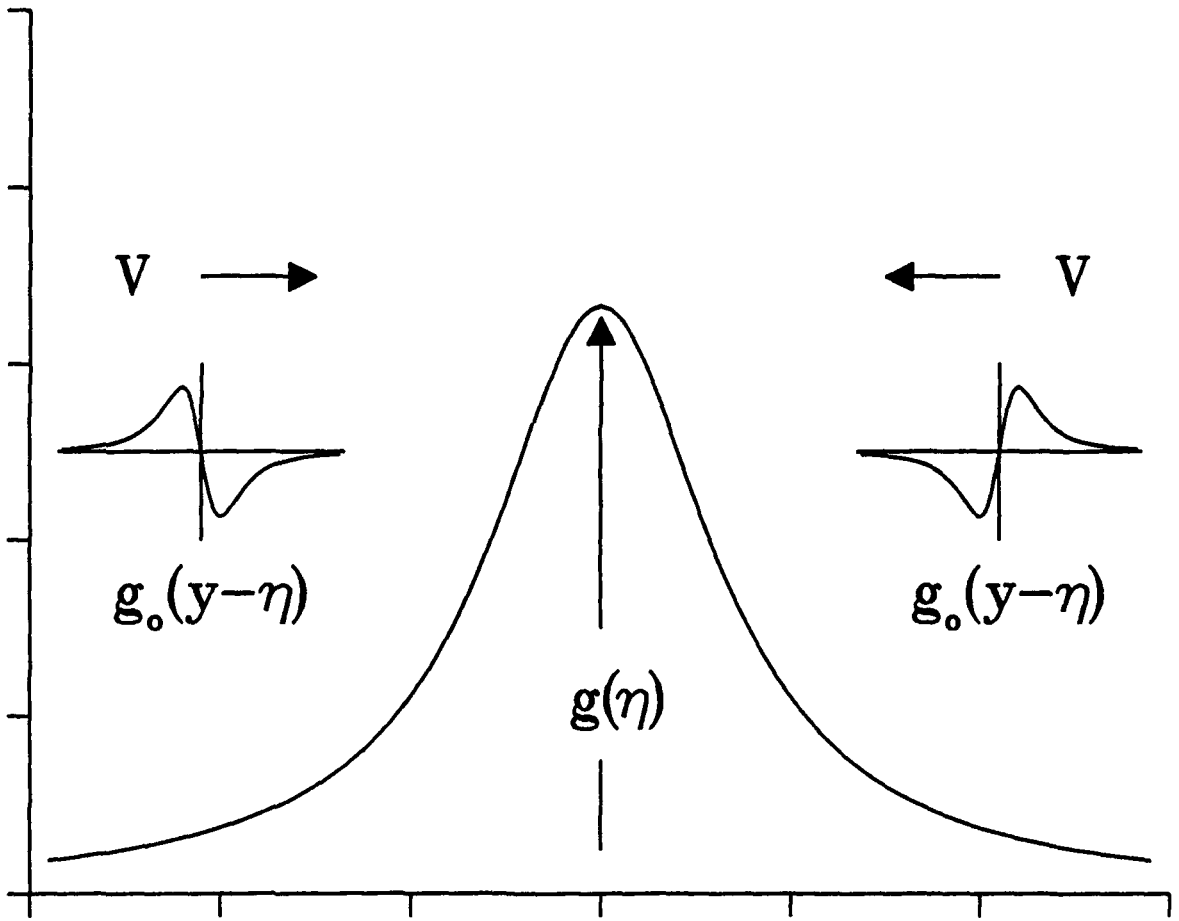

Figure 5. Entrainment velocities due to heat release, $f_\xi < 0$.

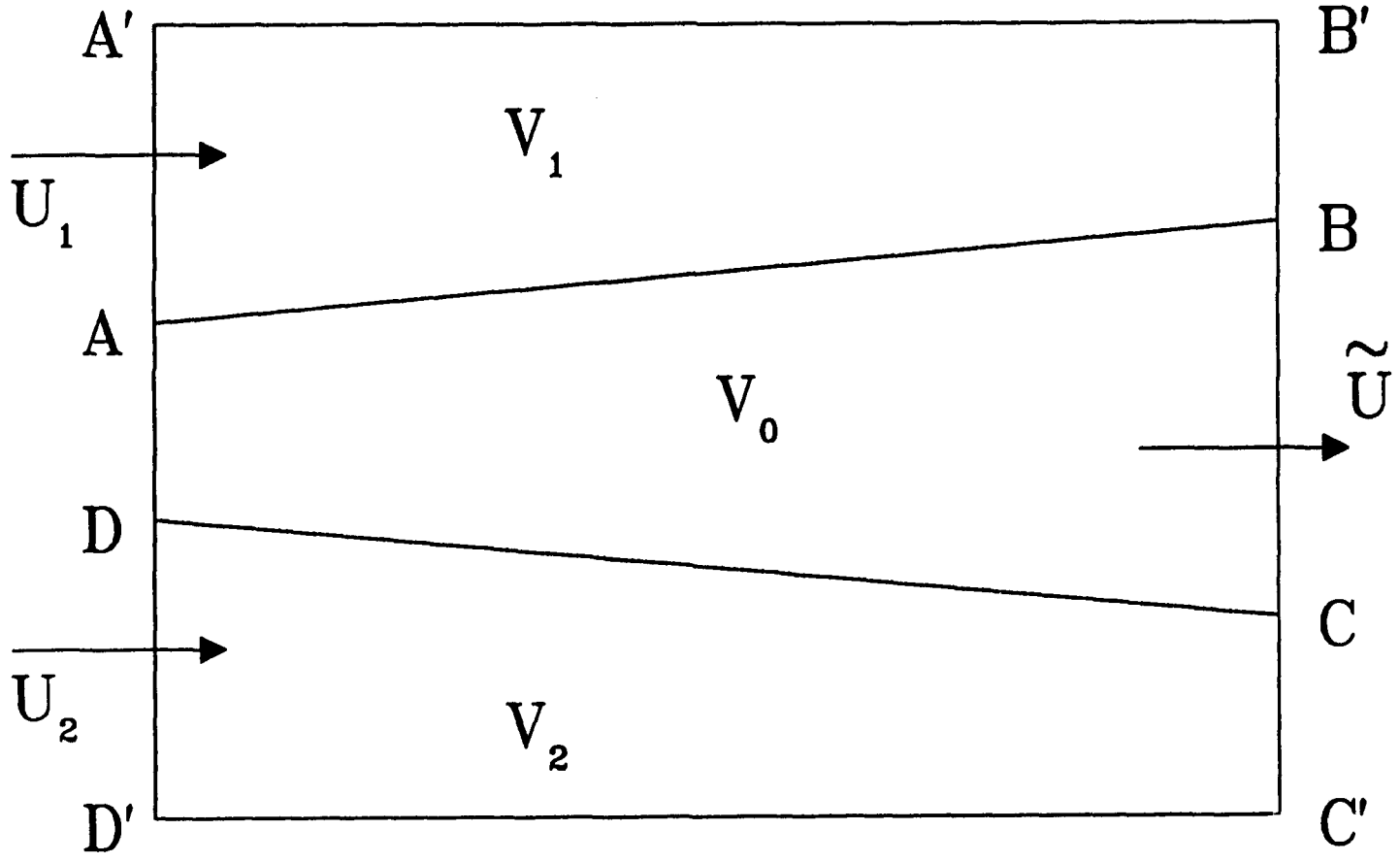

Figure 6. Control volume for energy balance in a shear layer.

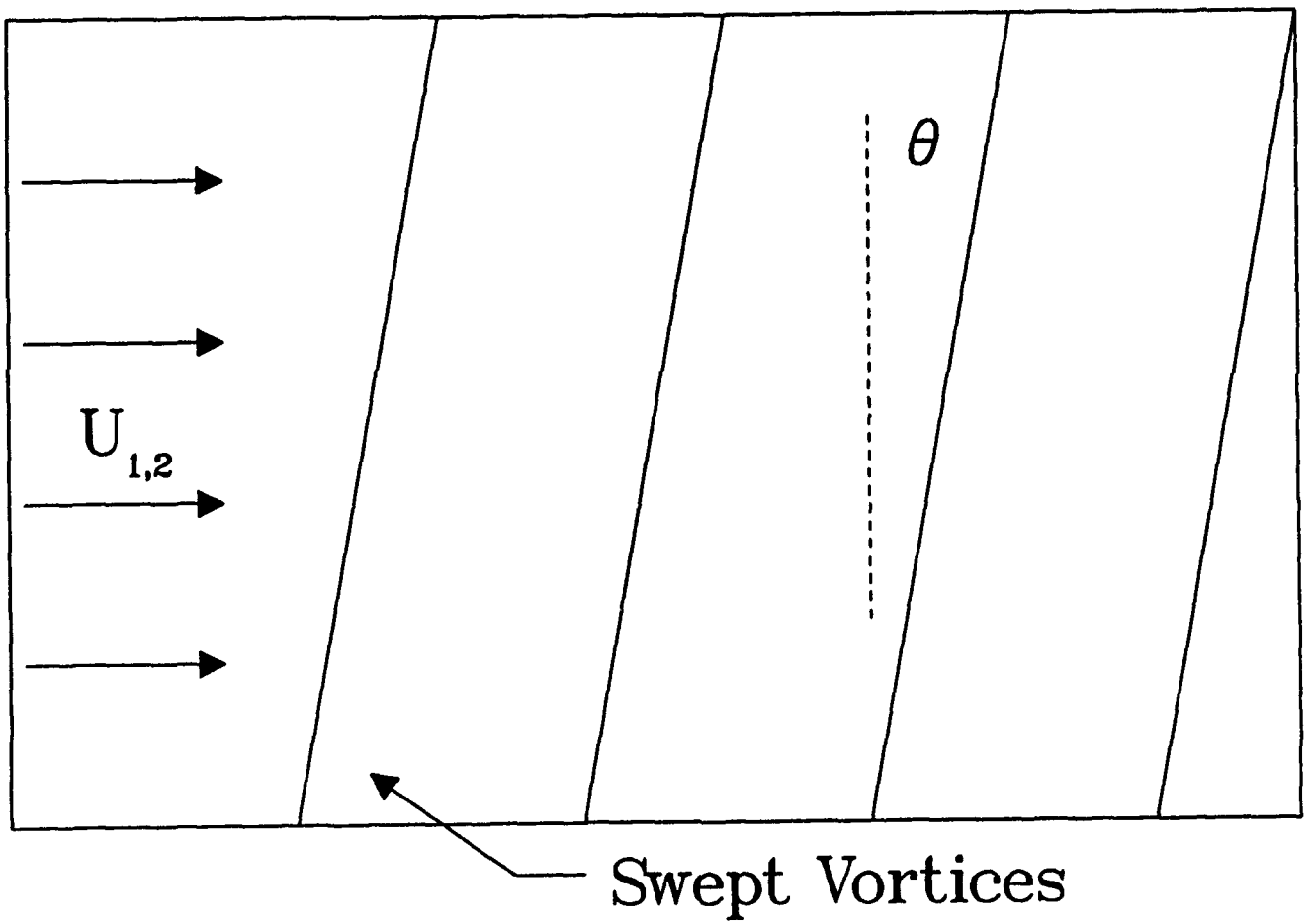

Figure 7. Swept vortices

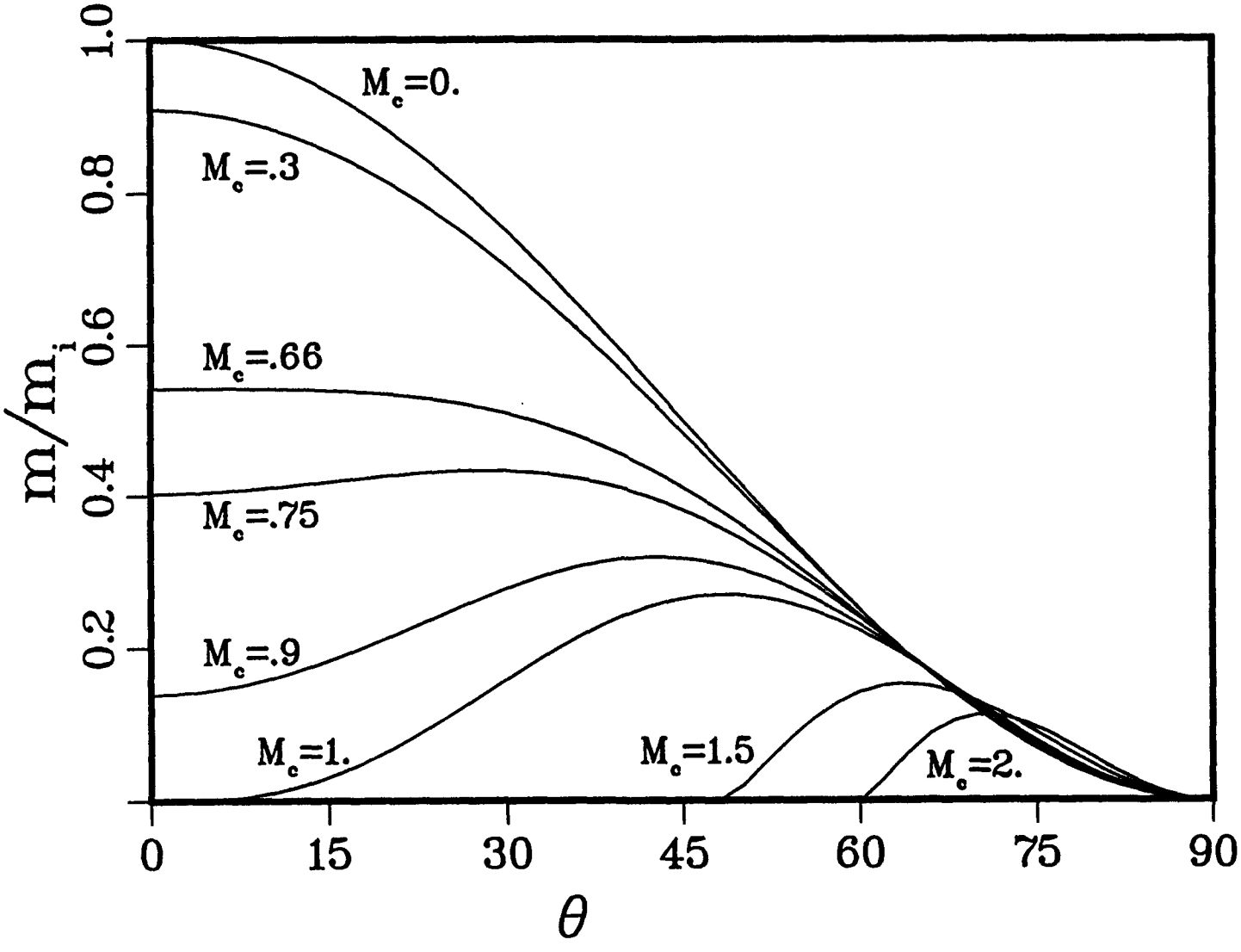

Figure 8. Mixing versus θ for various convective Mach numbers, M_c.

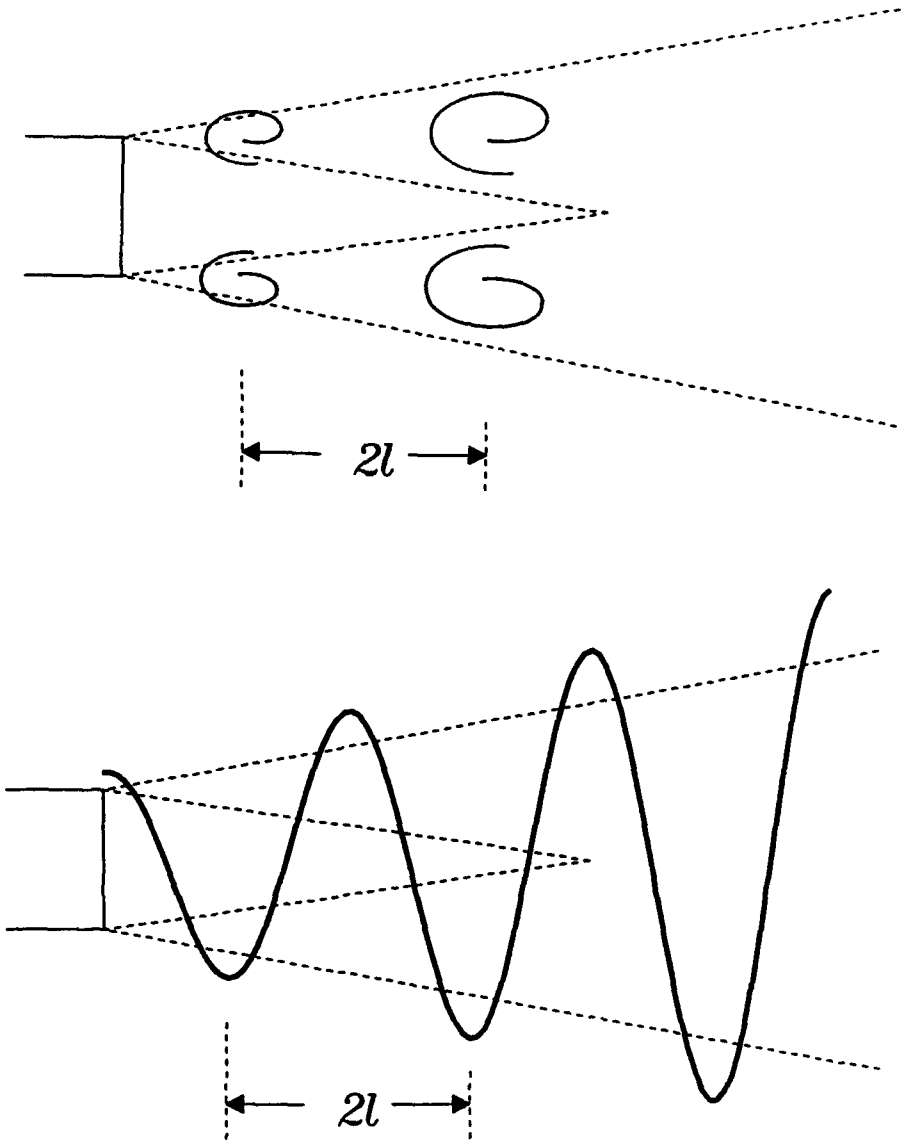

Figure 9. Possible jet vortex configurations.

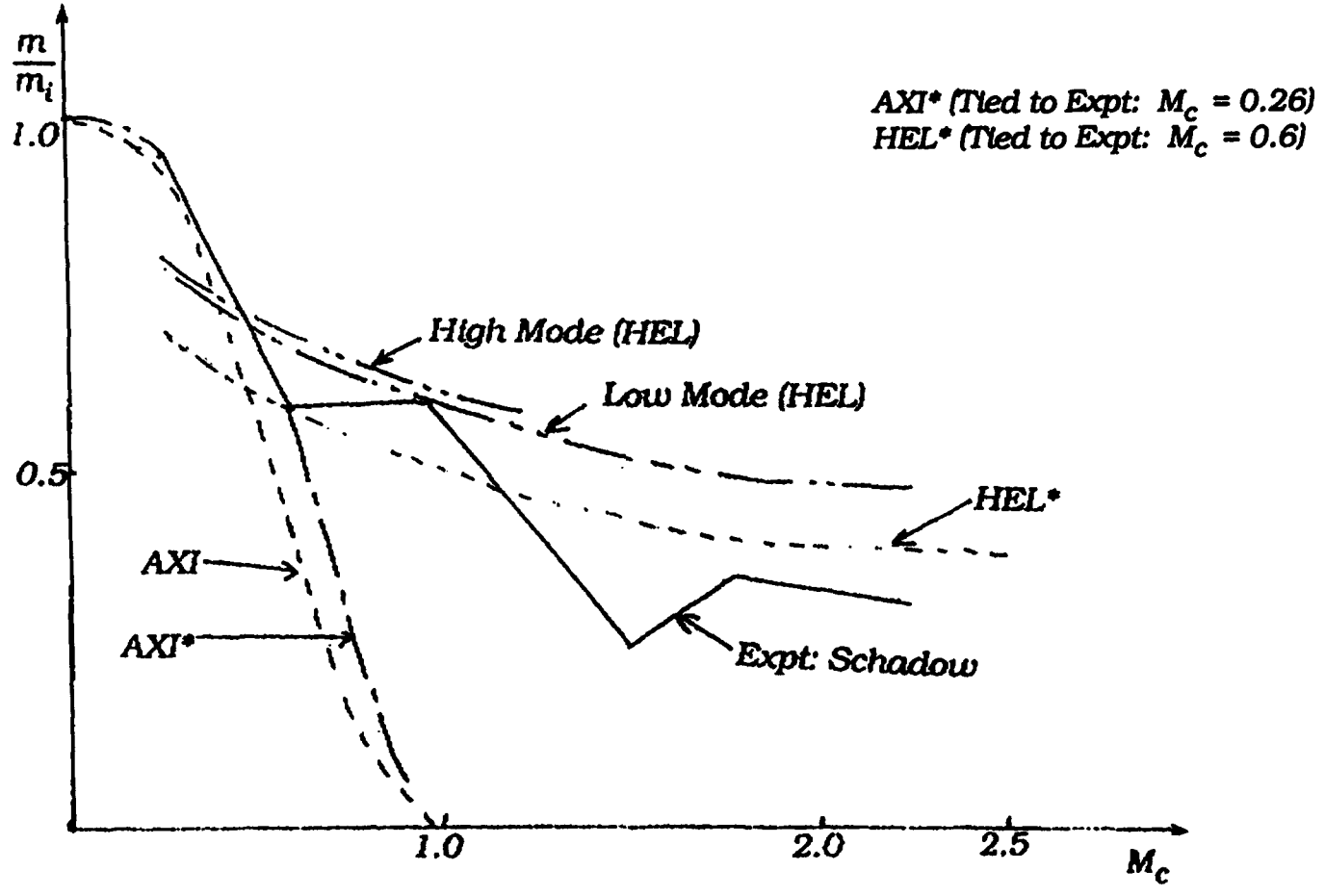

Figure 10. Mixing ratio vs convective Mach number in circular jets. Comparison between experiment and theory.